Journal of Applied Geophysics 108 (2014) 35–42

Contents lists available at ScienceDirect

Journal of Applied Geophysics

journal homepage: www.elsevier.com/locate/jappgeo

Edge detection of potential field data with improved structure tensor methods

Yuan Yuan [a,*], Danian Huang [a], Qinglu Yu [b], Pengyu Lu [c]

[a] College of Geo-exploration Science and Technology, Jilin University, Changchun, Jilin 130026, China
[b] Sinopec Geophysical Research Institute, Nanjing 211103, China
[c] College of Computer Science and Technology, Jilin University, Changchun, Jilin 130012, China

ARTICLE INFO

Article history:
Received 8 March 2014
Accepted 24 June 2014
Available online 1 July 2014

Keywords:
Potential field data
Structure tensor
Eigenvalue
Edge detection

ABSTRACT

Edge detection is a requisite task in the interpretation of potential field data. There are many methods based on horizontal and vertical derivative of potential field data for edge detection and enhancement. The large eigenvalue of structure tensor can well delineate the edges of geological bodies, but it cannot outline the edges of small amplitude geological bodies clearly. In order to overcome this problem, this paper proposes three different normalization methods to improve the edge detection ability of the large eigenvalue of structure tensor, so that they can display the large and small amplitude edges simultaneously. Also, they do not produce additional false edges when real geological bodies contain positive and negative anomalies simultaneously. These methods were tested on synthetic and measured gravity gradient data and magnetic data. All of the results have shown that the new improved methods are effective for edge detection.

1. Introduction

Edge detection plays an important role in the interpretation of potential-field data, which has been widely used as a tool in exploration technologies for mineral resources. Many filters are employed to detect and enhance the edges. The horizontal and vertical derivatives are often used to enhance the edge feature (Evjen, 1936; Cordell, 1979; Cordell and Grauch, 1985; Roest et al., 1992), which can only outline the edges of large amplitude anomalies. In order to display the large and small anomalies simultaneously, some balanced filters have been proposed (Cooper and Cowan, 2008; Ma and Li, 2012; Miller and Singh, 1994; Verduzco and Fairhead, 2004; Wijns et al., 2005).

Recently, eigenvalues of the potential field data have been used to delineate the edges of the geological bodies. Oruc et al. (2013) use the eigenvalues of curvature gravity gradient tensor to interpret the geological structure. Zhou et al. (2013) make some improvement on the method proposed by Oruc et al. (2013). The structure tensor is one of the image processing techniques and presents a local orientation in an n-dimensional space (Weickert, 1999a,b). Sertcelik and Kafadar (2012) use the large eigenvalue of structure tensor technique to extract the edges of causative bodies and the small eigenvalue to locate the corners of subsurface structures. The purpose of the Gaussian envelop used in the structure tensor is to smooth the potential field data and provide the corner information. Also, the Gaussian envelop can balance the amplitudes of different anomalies that consist of large and small anomalies with large value of the standard deviation. However, it cannot balance the amplitude completely.

Therefore, we propose three methods to balance the large eigenvalue of the structure tensor in this paper. We redefine the structure tensor without Gaussian envelops to avoid the potential field data too smooth. Also, the large eigenvalue outlines the edges of causative bodies.

2. Theory of the structure tensor

The redefined structure tensor matrix T without the Gaussian envelop is

$$T = \begin{bmatrix} \left(\frac{\partial f}{\partial x}\right)^2 & \frac{\partial f}{\partial x}\frac{\partial f}{\partial y} \\ \frac{\partial f}{\partial y}\frac{\partial f}{\partial x} & \left(\frac{\partial f}{\partial y}\right)^2 \end{bmatrix} = \begin{bmatrix} T_{11} & T_{12} \\ T_{21} & T_{22} \end{bmatrix}, \quad (1)$$

where f represents the original gravity anomaly or magnetic anomaly. $\frac{\partial f}{\partial x}$ and $\frac{\partial f}{\partial y}$ represent the derivatives of f in x and y directions. Each element in matrix T is a combination of the gradients of potential field.

The homogeneous characteristic equation for a 2D tensor T is

$$\lambda^2 - \lambda(T_{11} + T_{22}) + (T_{11}T_{22} - T_{12}T_{21}) = 0. \quad (2)$$

* Corresponding author. Tel.: +86 13844874863.
E-mail address: yuanyuan12@mails.jlu.edu.cn (Y. Yuan).

http://dx.doi.org/10.1016/j.jappgeo.2014.06.013
0926-9851/

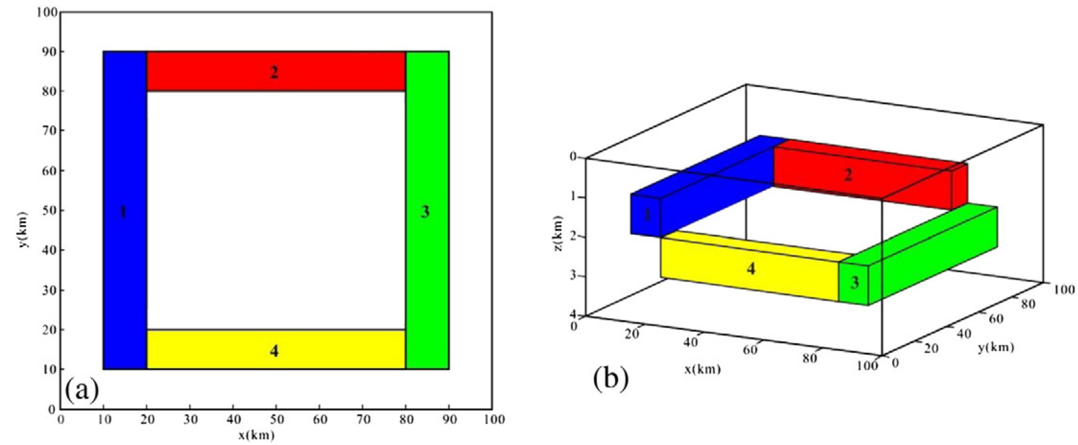

Fig. 1. Plan view and 3D view of synthetic model. (a) Plan view; (b) 3D view.

The large eigenvalue of matrix T is

$$\lambda_1 = \frac{1}{2}\left(T_{11} + T_{22} + \sqrt{(T_{11} - T_{22})^2 + 4T_{12}T_{21}}\right). \tag{3}$$

The maximum values of the eigenvalue λ_1 delineate the edges. However, it cannot display the large and small amplitudes simultaneously.

3. The improved methods for edge detection

In order to display the strong and small amplitude anomaly simultaneously, we present three normalization methods to balance the large eigenvalue.

Firstly, we use the square of the analytic signal of the potential field data to normalize the large eigenvalue, the expression is

$$NL_1 = \frac{\lambda_1}{\left(\frac{\partial f}{\partial x}\right)^2 + \left(\frac{\partial f}{\partial y}\right)^2 + \left(\frac{\partial f}{\partial z}\right)^2 + p \cdot \max(\lambda_1)}. \tag{4}$$

where p is a positive constant value decided by the interpreter. In general, the value of p is between 0.001 and 0.1. The introduction of p is to avoid producing additional false edges. The large value of p will reduce the effectiveness of balance, while the small value of p will enhance the edges of weak amplitude anomaly. The maximum values of NL_1 locate the edges.

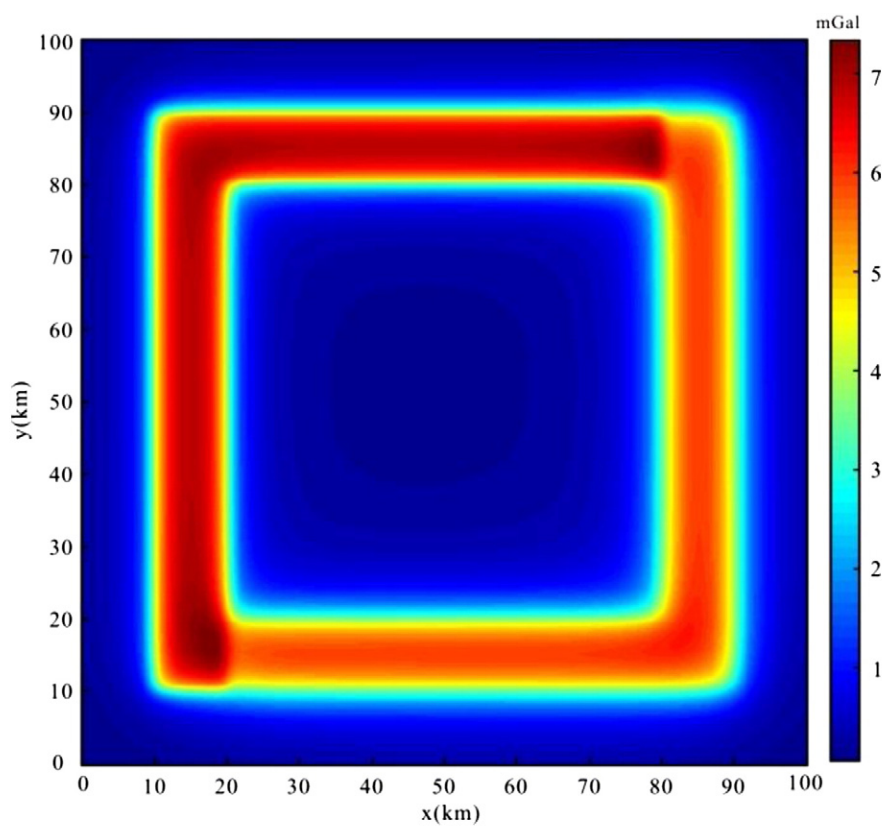

Fig. 2. Synthetic gravity anomaly model contains four vertical-sided prisms with top depths of 1 km (prism 1), 1 km (prism 2), 2 km (prism 3) and 2 km (prism 3). The contrasted densities of all prisms are 0.2 g/cm^3.